

Effective Mass of the Four Flux Composite Fermion at $\nu = 1/4$

W. Pan^{1,2}, H.L. Stormer^{3,4}, D.C. Tsui¹, L.N. Pfeiffer³, K.W. Baldwin³, and K.W. West³

¹*Princeton University, Princeton, New Jersey 08544*

²*NHMFL, Tallahassee, Florida 32310*

³*Lucent Technologies, Bell Laboratories, Murray Hill, New Jersey 07974*

⁴*Columbia University, New York, New York 10023*

(October 8, 2018)

We have measured the effective mass (m^*) of the four flux composite fermion at Landau level filling factor $\nu = 1/4$ (${}^4\text{CF}$), using the activation energy gaps at the fractional quantum Hall effect (FQHE) states $\nu = 2/7$, $3/11$, and $4/15$ and the temperature dependence of the Shubnikov-de Haas (SdH) oscillations around $\nu = 1/4$. We find that the energy gaps show a linear dependence on the effective magnetic field B_{eff} ($\equiv B - B_{\nu=1/4}$), and from this linear dependence we obtain $m^* = 1.0 m_e$ and a disorder broadening $\Gamma \sim 1$ K for a sample of density $n = 0.87 \times 10^{11} / \text{cm}^2$. The m^* deduced from the temperature dependence of the SdH effect shows large differences for $\nu > 1/4$ and $\nu < 1/4$. For $\nu > 1/4$, $m^* \sim 1.0 m_e$. It scales as $\sqrt{B_\nu}$ with the mass derived from the data around $\nu = 1/2$ and shows an increase in m^* as $\nu \rightarrow 1/4$, resembling the findings around $\nu = 1/2$. For $\nu < 1/4$, m^* increases rapidly with increasing B_{eff} and can be described by $m^*/m_e = -3.3 + 5.7 \times B_{eff}$. This anomalous dependence on B_{eff} is precursory to the formation of the insulating phase at still lower filling.

PACS Numbers: 73.40.Hm, 71.10.Pm

The composite fermion (CF) model has provided a unified view of the fractional quantum Hall effect (FQHE) sequences around the even denominator Landau level filling factors [1,2]. Closely related to Jain's wavefunction approach [3], Halperin, Lee, and Read [4] exploited a singular Chern-Simons gauge field transformation to explain the electronic transport properties at, or near, the even-denominator fillings. In this model, around the Landau level filling factor $\nu = 1/2\tilde{\phi}$ ($\tilde{\phi}$ is an integer), an even number $2\tilde{\phi}$ fictitious magnetic flux quanta are attached to each electron. The so formed composite particles, still preserving Fermi statistics, are named the composite fermions. By so doing, the strongly interacting two-dimensional electron system (2DES) in high magnetic (B) fields is transformed into an equivalent non- or weakly interacting CF system experiencing smaller effective B fields, $B_{eff} = B - B_{\nu=1/2\tilde{\phi}}$ ($B_{\nu=1/2\tilde{\phi}}$ is the B field at $\nu = 1/2\tilde{\phi}$). At $\nu = 1/2\tilde{\phi}$, where the attached flux quanta cancel exactly the external B field (or $B_{eff} = 0$), the CF's form a Fermi sea. This Fermi system has an effective mass (m^*) dependent only on the electron-electron ($e-e$) interaction, which is proportional to $e^2/\epsilon l_B$, where ϵ is the dielectric constant of GaAs and the magnetic length $l_B = (\hbar c/eB_\nu)^{1/2}$. Thus $m^* \propto \sqrt{B_\nu}$. When the cancellation is not exact, the CF's see B_{eff} and follow the semiclassical cyclotron orbits. At large B_{eff} , cyclotron orbits of the CF's are quantized and the energy spectrum of the CF's breaks up into discrete Landau levels. The CF Landau level filling factor p is related to the electron Landau level filling factor ν through

$$\nu = \frac{p}{2\tilde{\phi}p \pm 1}, \quad (1)$$

where $p = 1, 2, 3, \dots$.

The above picture was supported by the experiments around $\nu = 1/2$ ($\tilde{\phi} = 1$) [5–15]. In particular, the activation energy measurement [9] of the prominent FQHE sequences $\nu = \frac{p}{2p \pm 1}$ showed that the energy gaps of the FQHE states in each sequence showed a strikingly linear dependence on B_{eff} emanating from $B_{\nu=1/2}$ (the B field at $\nu = 1/2$), consistent with the formation of CF's at $\nu = 1/2$ (${}^2\text{CF}$'s). From this linear dependence an effective mass, m^* , about one magnitude larger than the bare 2DES mass was obtained for the CF's [9]. The Shubnikov-de Haas (SdH) formalism [9–12] was also adopted to determine m^* and the scattering time of ${}^2\text{CF}$'s. It was found from this analysis that m^* was nearly constant for large positive and negative B_{eff} , showed a B_{eff} dependent enhancement for smaller B_{eff} , and divergent as $B_{eff} \rightarrow 0$.

The focus of all earlier experiments was on the ${}^2\text{CF}$'s around $\nu = 1/2$ or around $\nu = 3/2$ [13]. Other even-denominator filling factors, such as $\nu = 1/4$ ($\tilde{\phi} = 2$), was not fully addressed. In particular, will the CF's form at $\nu = 1/4$? It is believed that Wigner crystal is the preferred ground state for $\nu < 1/5$. If the CF's do form at $\nu = 1/4$ (${}^4\text{CF}$'s), how do they compare to the ${}^2\text{CF}$'s? So far, only a few preliminary experimental results about $\nu = 1/4$ exist in the literature [9,10,14]. The recent study carried out by Yeh *et al.* [15] concentrated on the ${}^4\text{CF}$'s at $\nu = 3/4$, the particle-hole conjugate of $\nu = 1/4$. It should be apparent that this lack of experiments on the ${}^4\text{CF}$'s is mainly due to the fact that such an experiment is far more demanding. To resolve the FQHE sequences $\nu = \frac{p}{4p \pm 1}$ around $\nu = 1/4$ requires much higher quality samples and higher B fields.

We wish to report in this paper a systematic study of the ${}^4\text{CF}$'s at $\nu = 1/4$. We find that the energy gaps of the prominent FQHE states above $\nu = 1/4$, *i.e.*, at $\nu = 2/7, 3/11$, and $4/15$, show a linear dependence on B_{eff} ($\equiv B - B_{\nu=1/4}$). From this linear dependence we obtain an effective mass $m^*/m_e = 1.0$, where m_e is the bare electron mass, and a disorder broadening $\Gamma \sim 1$ K for a sample of density $n = 0.87 \times 10^{11} \text{ /cm}^2$. We have also studied the temperature dependence of the $\nu = \frac{p}{4p \pm 1}$ FQHE series as that of the SdH effect of the ${}^4\text{CF}$'s and determined m^* as a function of B_{eff} on both sides of $\nu = 1/4$. The m^* deduced from the data taken for $B_{eff} < 0$ and from those taken for $B_{eff} > 0$ differs considerably. For large negative B_{eff} (≤ -1.0 T), m^* is nearly constant ($m^*/m_e \sim 1.0$), in agreement with that from the activation measurement. It scales as $\sqrt{B_\nu}$ with the mass derived from the data at lower B field around $\nu = 1/2$. An increase in m^* is observed as $B_{eff} \rightarrow 0$, resembling the findings around $\nu = 1/2$. However, for $B_{eff} > 0$, m^* increases rapidly with B_{eff} and can be described by $m^*/m_e = -3.3 + 5.7 \times B_{eff}$ (B_{eff} in Tesla). We believe that this anomalous linear dependence on B_{eff} is related to the formation of the insulating phase at still higher B , or smaller ν .

We have investigated three samples (A, B, and C in Table I) from three different wafers. The samples are GaAs/AlGaAs heterostructures of electron densities $n = (0.87, 0.85, 0.65) \times 10^{11} \text{ /cm}^2$ and mobilities $\mu = (10.5, 8.2, 6.6) \times 10^6 \text{ cm}^2/\text{Vs}$, respectively, after illumination by a red light-emitting diode (LED) at 4.2 K. The size of each sample is about $5 \text{ mm} \times 5 \text{ mm}$ with eight indium contacts placed symmetrically around the edges, four at the corners and four in the centers of the four edges. A standard low-frequency ($\sim 5 \text{ Hz}$) lock-in technique was employed to measure the transport coefficients, using an excitation current varying from 0.1 nA to 1 nA. A calibrated RuO_2 thermometer of known corrections for magnetoresistance was mounted next to the sample for the temperature (T) measurement. The experiments were performed in a top-loading dilution refrigerator with T down to 20 mK and B up to 18 T.

Fig. 1 shows the diagonal resistance R_{xx} vs. B around $\nu = 1/4$ for sample A. The exceptional sample quality is manifested by the appearance of the higher order FQHE states at $\nu = 5/19, 4/17$ and a very low resistance at $\nu = 1/5$. R_{xx} has been measured at many temperatures, and here we show two different temperature traces taken at $T = 25$ and 150 mK. The FQHE states at $\nu = 2/7, 3/11$, and $4/15$ above $\nu = 1/4$ and at $\nu = 2/9$ below $\nu = 1/4$ exhibit the typical quantum Hall liquid characteristic — the resistance minima decrease with decreasing T . The activation gap Δ is obtained from the T dependence of R_{xx} through $R_{xx} \propto \exp(-\Delta/2k_B T)$. In the inset, the activation gaps at $2/7, 3/11$, and $4/15$ are plotted against $B_{eff} = B - B_{\nu=1/4}$. They show a linear dependence on B_{eff} with a negative intercept Γ at $B_{eff} = 0$. This linear dependence, as expected for the ${}^4\text{CF}$'s at $\nu = 1/4$, allows

us to obtain an effective mass, $m^*/m_e = 1.0$, from the slope of the line via the equation $\Delta = \hbar e B_{eff} / m^* c - \Gamma$ [4,9]. The negative intercept at $B_{eff} = 0$ gives the disorder broadening of the CF Landau level, $\Gamma \sim 1$ K.

We have also studied the T dependence of the $\nu = \frac{p}{4p \pm 1}$ FQHE series as that of the SdH effect of the ${}^4\text{CF}$'s and deduced m^* on both sides of $\nu = 1/4$ [9–12]. The amplitude of the SdH oscillations (ΔR) is obtained following the standard method [9], and is fitted by a nonlinear least-square technique according to the following equation

$$\frac{\Delta R}{R_0} \propto \frac{\xi}{\sinh(\xi)}, \quad (2)$$

where $\xi = 2\pi^2 k_B T / \hbar \omega_c^* = 2\pi^2 k_B T m^* c / e \hbar B_{eff}$, ω_c^* is the cyclotron frequency, and m^* is the effective mass. R_0 is the diagonal resistance at $B_{eff} = 0$. All other symbols have their usual meanings. In the fitting, it has been assumed that the relaxation time τ of the ${}^4\text{CF}$'s is temperature independent.

Since $m^* \propto \sqrt{B_\nu}$, we introduce a normalized mass, $m_{nor}^* = m^* / \sqrt{B_\nu}$, to take into account of the sample density differences. Here m^* is in units of m_e and B_ν is the magnetic field at which $B_{eff} = 0$, in units of T. In Fig. 2, m_{nor}^* for the CF's at $\nu = 1/4$ is plotted as a function of B_{eff} for all three samples: solid squares for sample A, open circles for B, and open diamonds for C. We also include the m_{nor}^* for the ${}^4\text{CF}$'s at $\nu = 3/4$ from samples D, E, and F of Yeh *et al.* [15] (noting that $B_{eff} = -3 \times (B - B_{\nu=3/4})$ for the ${}^4\text{CF}$'s around $\nu = 3/4$). In Table I we summarize the sample parameters for all six samples. Despite the large differences in n and μ , the normalized ${}^4\text{CF}$ mass behaves very similarly: $m_{nor}^* \sim 0.26$ for $B_{eff} \leq -1.0$ T, increases to ~ 0.33 at $B_{eff} = -0.7$ T, and tends to diverge as $B_{eff} \rightarrow 0$, similar to the findings for ${}^2\text{CF}$'s. For $B_{eff} > 0$, m_{nor}^* is anomalously large. It shows a linear dependence on B_{eff} and can be fitted to $m_{nor}^* = -0.88 + 1.5 \times B_{eff}$, independent of n and μ and whether it is measured around $\nu = 1/4$ or $\nu = 3/4$.

It is clear from Fig. 1 that the $\nu = \frac{p}{4p \pm 1}$ FQHE features in R_{xx} vs. B show a large asymmetry across $\nu = 1/4$, and for $\nu < 1/4$, a strong T dependent background is observed to increase steeply with increasing B . The huge R_{xx} peak ($\sim 4 \text{ M}\Omega$) between $\nu = 2/9$ and $\nu = 1/5$ is due to the reentrant insulating behavior attributed to the formation of a pinned Wigner solid [16]. Hence, it is not surprising that the ${}^4\text{CF}$ mass deduced from the T dependence of the $\nu = \frac{p}{4p \pm 1}$ FQHE features is anomalous, and it is natural to associate the observed asymmetry in m^* vs. B_{eff} with the formation of the insulating phase at still lower filling factors. It should also be noted that anomalously large ${}^4\text{CF}$ m^* was previously deduced from the $\nu = 4/5$ FQHE data, and it was believed to be a consequence of the influence of hole localization of the electron-hole symmetric state at $\nu = 4/5$. In any case, the m^* in Table I is the ${}^4\text{CF}$ mass obtained at large negative B_{eff} around $\nu = 1/4$ and $3/4$.

We have also calculated m^* at $\nu = 2/7$ for sample A following the mean field theory [4], which relates m^* to the Coulomb energy $e^2/\epsilon l_B$ via $\hbar e B_{eff}/m^*c = g^\nu e^2/\epsilon l_B$. Here g^ν is a constant at ν [17–20] and we used $g^{\nu=2/7} = 0.024$ from Ref. 20. m^* was found, after corrected for the finite thickness of the 2DES [21], to be $0.9 m_e$, very close to the measured value of $1.0 m_e$.

We now turn to the comparison between the ^4CF 's and the ^2CF 's. For this purpose, we measured the SdH m^* of the ^2CF 's of sample A, and plotted them as the solid circles in Fig. 3. The solid squares are the ^4CF data for $B_{eff} < 0$ of the same sample. The ^4CF data for $B_{eff} > 0$ are not included. We also include the ^2CF data from Refs. 9 and 12; they are represented by the open symbols — squares, circles, dot-centered up-triangles, and cross-centered down-triangles. Two important results emerge from Fig. 3. First, the m_{nor}^* 's for ^4CF and ^2CF from the same sample are of the same magnitude within our experimental error and show a similar dependence on B_{eff} . So far we are not aware of any theories predicting a same value of m^* for the ^2CF 's and ^4CF 's. On the contrary, if we regard the $\nu = 1/4$ state as the $\nu = 1/2$ state of CF's emanating from $\nu = 1/2$, we would have expected to see different m^* 's. Second, the ^2CF mass from different samples with different n and μ , varying from $n = 0.87 \times 10^{11}/\text{cm}^2$ to $2.3 \times 10^{11}/\text{cm}^2$ and $\mu = 2.5 \times 10^6 \text{ cm}^2/\text{Vs}$ to $12.8 \times 10^6 \text{ cm}^2/\text{Vs}$, also shows a similar dependence on B_{eff} . The large spread in magnitude is to be expected in view of the large difference in disorder in the different samples as seen in the spread in their mobilities.

In summary, we have measured the ^4CF effective mass using the activation energy gaps at the FQHE states $\nu = 2/7, 3/11$, and $4/15$, and the temperature dependence of the SdH oscillations around $\nu = 1/4$. We find that the energy gaps show a linear dependence on B_{eff} , and from this linear dependence we obtain $m^* = 1.0 m_e$ and a disorder broadening $\Gamma \sim 1 \text{ K}$. The m^* deduced from the T dependence of the SdH effect shows an asymmetry for the negative and positive B_{eff} . For $B_{eff} < 0$, $m^* \sim 1.0 m_e$ for large negative B_{eff} ($\leq -1.0 \text{ T}$), shows a B_{eff} dependent enhancement for smaller B_{eff} , and divergent as $B_{eff} \rightarrow 0$. It scales as $\sqrt{B_\nu}$ with the mass derived from the data around $\nu = 1/2$ and $3/4$. For $B_{eff} > 0$, m^* is anomalously large and shows a linear dependence on B_{eff} . This behavior is believed to be related to the formation of Wigner crystal phase at still lower filling factor.

We thank E. Palm and T. Murphy for the experimental assistance, and A.S. Yeh, R.R. Du, and N.E. Bonesteel for discussions. A portion of this work was performed at the National High Magnetic Field Laboratory which is supported by NSF Cooperative Agreement No. DMR-9527035 and by the State of Florida. D.C.T. and W.P. are supported by the DOE and the NSF.

- [1] *Perspectives in Quantum Hall Effects* edited by S. Das Sarma and A. Pinczuk (Wiley, New York, 1996).
- [2] *Composite Fermions: A Unified View of the Quantum Hall Regime* edited by O. Heinonen (World Scientific, Singapore, 1998).
- [3] J.K. Jain, Phys. Rev. Lett. **63**, 199 (1989); Phys. Rev. B **41**, 7653 (1990); Science **266**, 1199 (1994).
- [4] B.I. Halperin, P.A. Lee, and N. Read, Phys. Rev. B **47**, 7312 (1993).
- [5] R.L. Willett, R.R. Ruel, K.W. West, and L.N. Pfeiffer, Phys. Rev. Lett. **71**, 3846 (1993).
- [6] W. Kang, H.L. Stormer, L.N. Pfeiffer, K.W. Baldwin, and K.W. West, Phys. Rev. Lett. **71**, 3850 (1993).
- [7] V.J. Goldman, B. Su, and J.K. Jain, Phys. Rev. Lett. **72**, 2065 (1994).
- [8] J.H. Smet, D. Weiss, R.H. Lutjering, K. von Klitzing, R. Fleishmann, R. Ketmerick, T. Geisel, and G. Weimann, Phys. Rev. Lett. **77**, 2272 (1996).
- [9] R.R. Du, H.L. Stormer, D.C. Tsui, L.N. Pfeiffer, and K.W. West, Phys. Rev. Lett. **70**, 2944 (1993); *ibid.* **73**, 3274 (1994); Solid State Communications **90**, 71 (1994).
- [10] D.R. Leadley, R.J. Nicholas, C.T. Foxon, and J.J. Harris, Phys. Rev. Lett. **72**, 1906 (1994).
- [11] H.C. Manoharan, M. Shayegan, and S.J. Klepper, Phys. Rev. Lett. **73**, 3270 (1994).
- [12] P.T. Coleridge, Z.W. Wasilewski, P. Zawadzki, A.S. Sachrajda, and H.A. Carmona, Phys. Rev. B **52**, 11603 (1995).
- [13] R.R. Du, A.S. Yeh, H.L. Stormer, D.C. Tsui, L.N. Pfeiffer, and K.W. West, Phys. Rev. Lett. **75**, 3926 (1995).
- [14] R.L. Willett and L.N. Pfeiffer, Surface Science **361/362**, 38 (1996).
- [15] A.S. Yeh, H.L. Stormer, D.C. Tsui, L.N. Pfeiffer, K.W. Baldwin, and K.W. West, Phys. Rev. Lett. **82**, 592 (1999).
- [16] H.W. Jiang, R.L. Willett, H.L. Stormer, D.C. Tsui, L.N. Pfeiffer, and K.W. West, Phys. Rev. Lett. **65**, 633 (1990); R.R. Du, D.C. Tsui, H.L. Stormer, L.N. Pfeiffer, and K.W. West, Solid State Communications **99**, 755 (1996).
- [17] G. Fano, F. Ortolani, and E. Colombo, Phys. Rev. B **34**, 2670 (1986).
- [18] T. Chakraborty and P. Pietiläinen, *The Fractional Quantum Hall Effect*, Springer Series in solid State Science **85** (Springer-Verlag, New York, 1988).
- [19] N. d'Ambrumenil and R. Morf, Phys. Rev. B **40**, 6108 (1989).
- [20] N.E. Bonesteel, Phys. Rev. B **51**, 9917 (1995).
- [21] F.C. Zhang and S. Das Sarma, Phys. Rev. B **33**, 2903 (1986).

TABLE I. The density n and the mobility μ for samples (A, B, C) and (D, E, F)¹⁵, and the effective mass m^* for ⁴CF measured around $\nu = 1/4$ and $\nu = 3/4$. m^* is in units of the bare electron mass.

sample	n ($10^{11}/\text{cm}^2$)	μ ($10^6 \text{ cm}^2/\text{Vs}$)	m^*	m_{nor}^*
A (03-14-97-1A)	0.87	10.5	1.0	0.27
B (03-27-97-1A)	0.85	8.2	1.0	0.27
C (03-27-97-2A)	0.65	6.6	0.90	0.29
D (02-03-97-1A)	0.86	11.0	0.58	0.26
E (10-19-91-1A)	1.13	6.8		
F (12-06-91-1A)	2.26	13.0	0.90	0.25

Fig. 1 Pan et al.

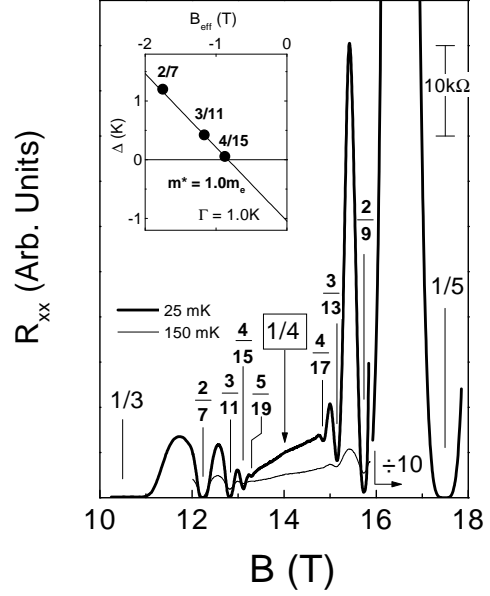


FIG. 1. R_{xx} vs. B around $\nu = 1/4$ for sample A. The vertical lines mark the positions of filling factor ν . Two traces at 25 mK (thick line) and 150 mK (thin line) are shown to illustrate the temperature dependence of R_{xx} . The inset shows the plot of the activation gap Δ vs. B_{eff} at $\nu = 2/7$, $3/11$, and $4/15$. The straight line is a linear fit to the experimental data. m^* is the effective mass of the ⁴CF's obtained from the activation measurement. Γ is the disorder broadening.

Fig. 2 Pan et al.

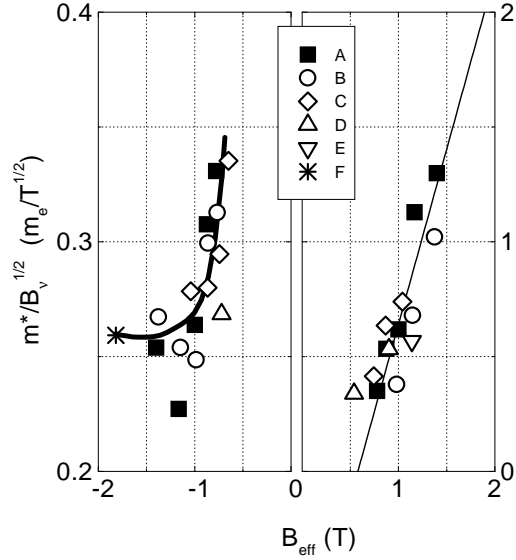


FIG. 2. m_{nor}^* vs. B_{eff} around $\nu = 1/4$ for sample A (solid squares), B (open circles), and C (open diamonds). The results around $\nu = 3/4$ obtained by Yeh *et al.*¹⁵ for sample D (open up-triangles), E (open down-triangle), and F (aster) are also included. The gray line is guide to the eye and the straight line is a linear fit to the data. m^* is in units of m_e . B_v is the B field where the CF's form, in units of T.

Fig. 3 Pan et al.

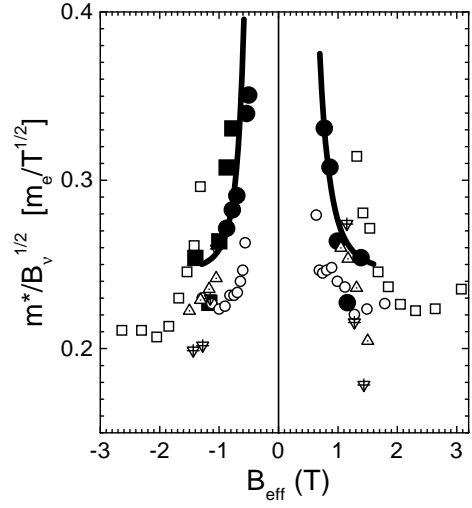


FIG. 3. Comparison of m_{nor}^* of the ^4CF 's and the ^2CF 's. The solid squares and solid circles represent m_{nor}^* for ^4CF and ^2CF respectively of sample A. The gray lines are guides to the eye. The open symbols (\square , \circ , \triangle , and ∇) represent the ^2CF data obtained by Du *et al.*⁹ and Coleridge *et al.*¹² for their samples of densities $(2.3, 1.13, 1.27, \text{ and } 1.39) \times 10^{11} \text{ cm}^{-2}$ and mobilities $(12.8, 6.8, 3.5, \text{ and } 2.5) \times 10^6 \text{ cm}^2/\text{Vs}$, respectively. m^* is in units of m_e and B_v in T.